Electronic Supplementary Material (ESI) for Physical Chemistry Chemical Physics.

Supporting Information: Solvent Effects on Extractant Conformational Energetics in Liquid-Liquid Extraction: A Simulation Study of Molecular Solvents and Ionic Liquids

Xiaoyu Wang,* Srikanth Nayak, Richard E. Wilson, L. Soderholm, and Michael J. Servis*

Chemical Sciences and Engineering Division, Argonne National Laboratory, 9700 S Cass Ave, Lemont, IL 60439

E-mail: xiaoyu.wang@anl.gov; mservis@anl.gov

Table S1: Frequency of C=O stretching (cm^{-1}) from literature and DFT (this work)

	non-binding CMPO	binding CMPO	shift
DFT[a]	1659	1558	101
Exptl.[b]	∼1640	∼1600	∼40

[a] DFT IR peaks are scaled by an empirical value of 0.95, which is suggested from https://cccbdb.nist.gov/vibscalejust.asp.

[b] From Tkac et al.'s work[1]

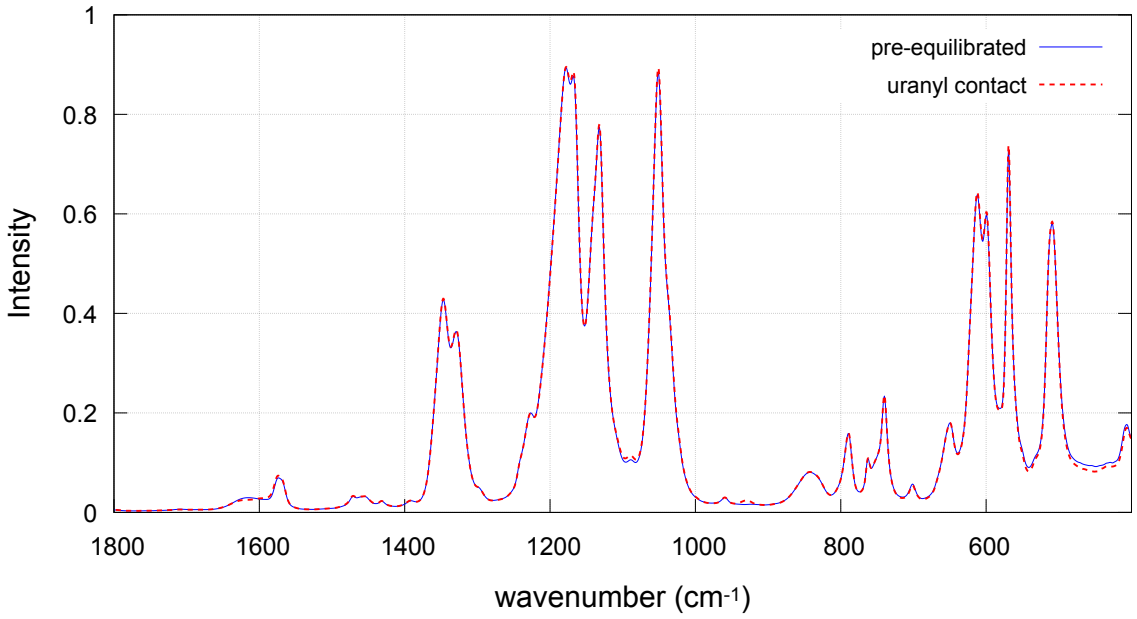

Figure S1: IR spectra for 0.1 M CMPO in [EMIM][Tf_2N] for the pre-equibrated organic phase (solid line) and uranyl-contacted organic phase (dashed line).

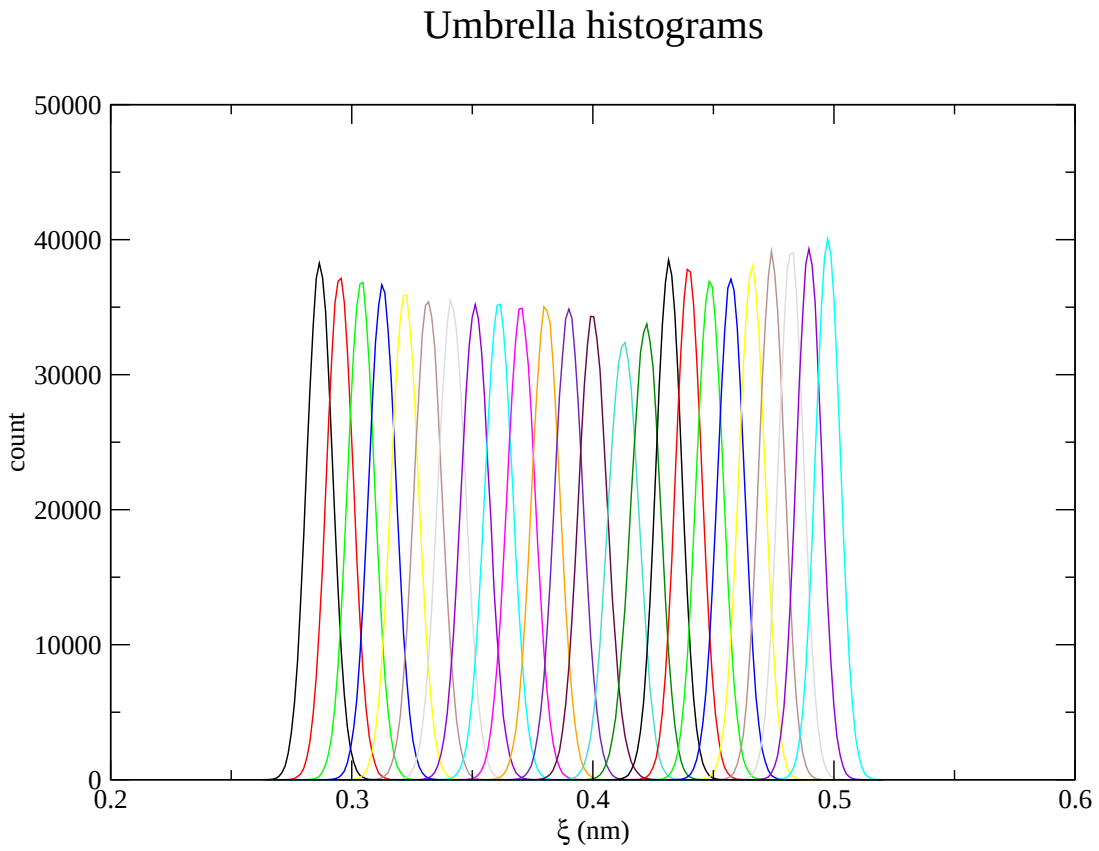

Figure S2: Histrograms of the collective variable in vacuum, O(=P) to O(=C) distance (Å), in each window along the reaction coordinate.

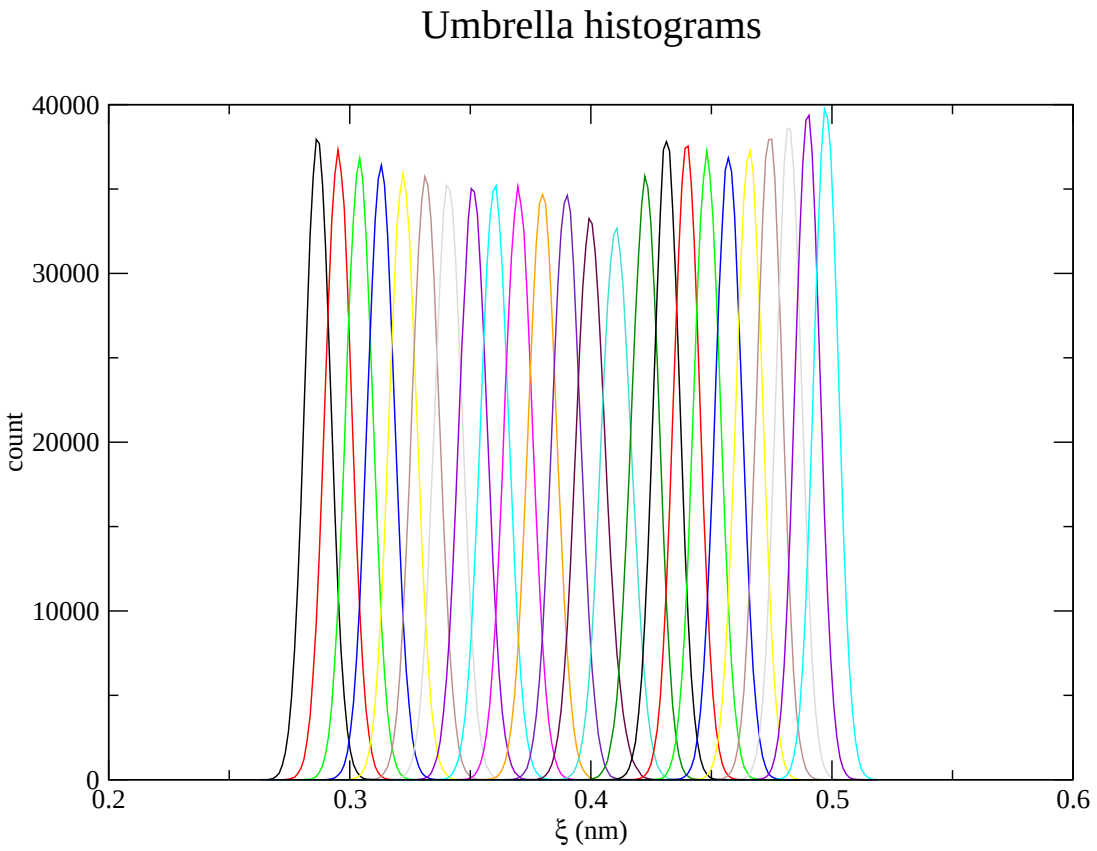

Figure S3: Histrograms of the collective variable in dodecane, O(=P) to O(=C) distance (Å), in each window along the reaction coordinate.

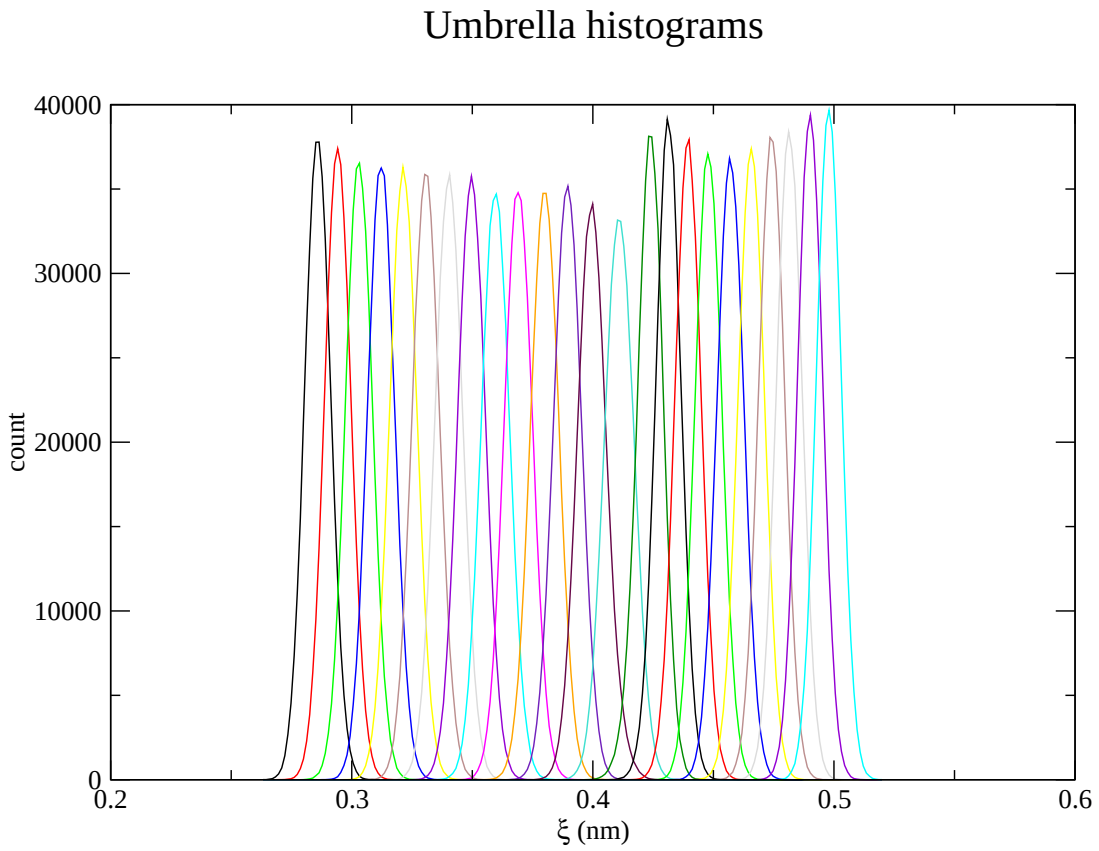

Figure S4: Histrograms of the collective variable in TBP, O(=P) to O(=C) distance (Å), in each window along the reaction coordinate.

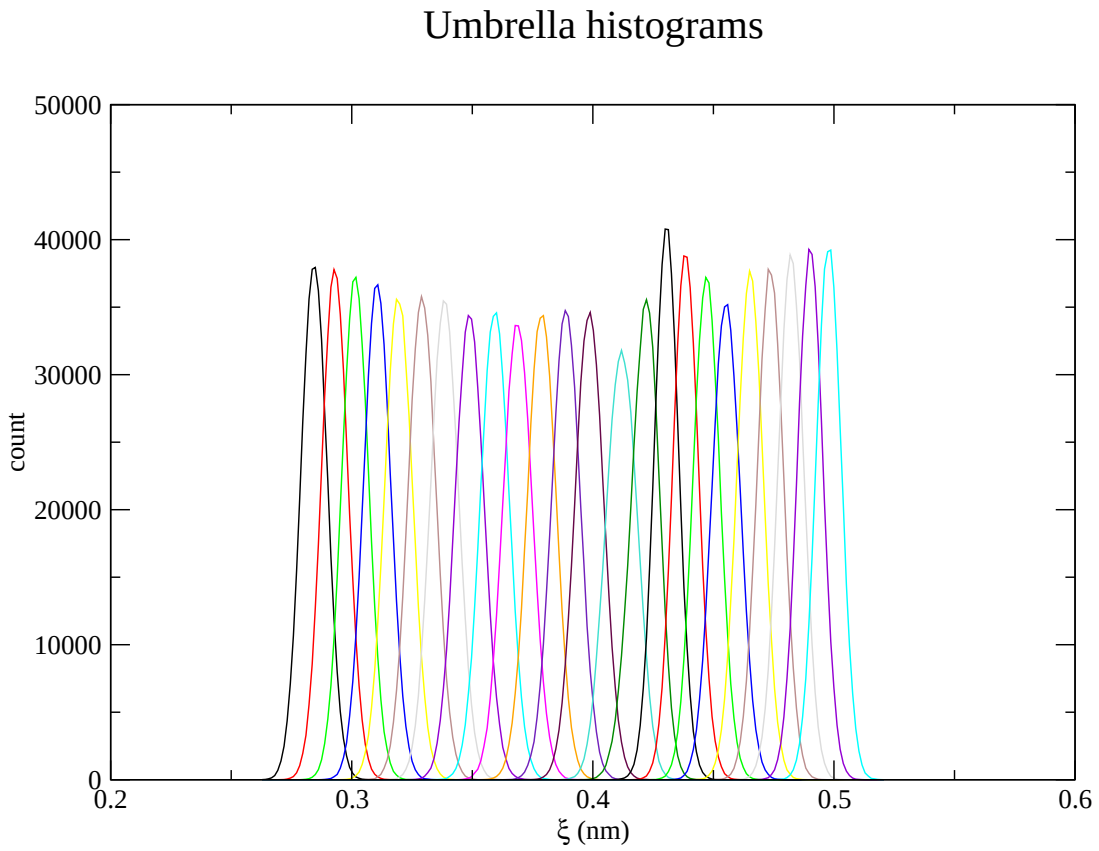

Figure S5: Histrograms of the collective variable in dry IL, O(=P) to O(=C) distance (Å), in each window along the reaction coordinate.

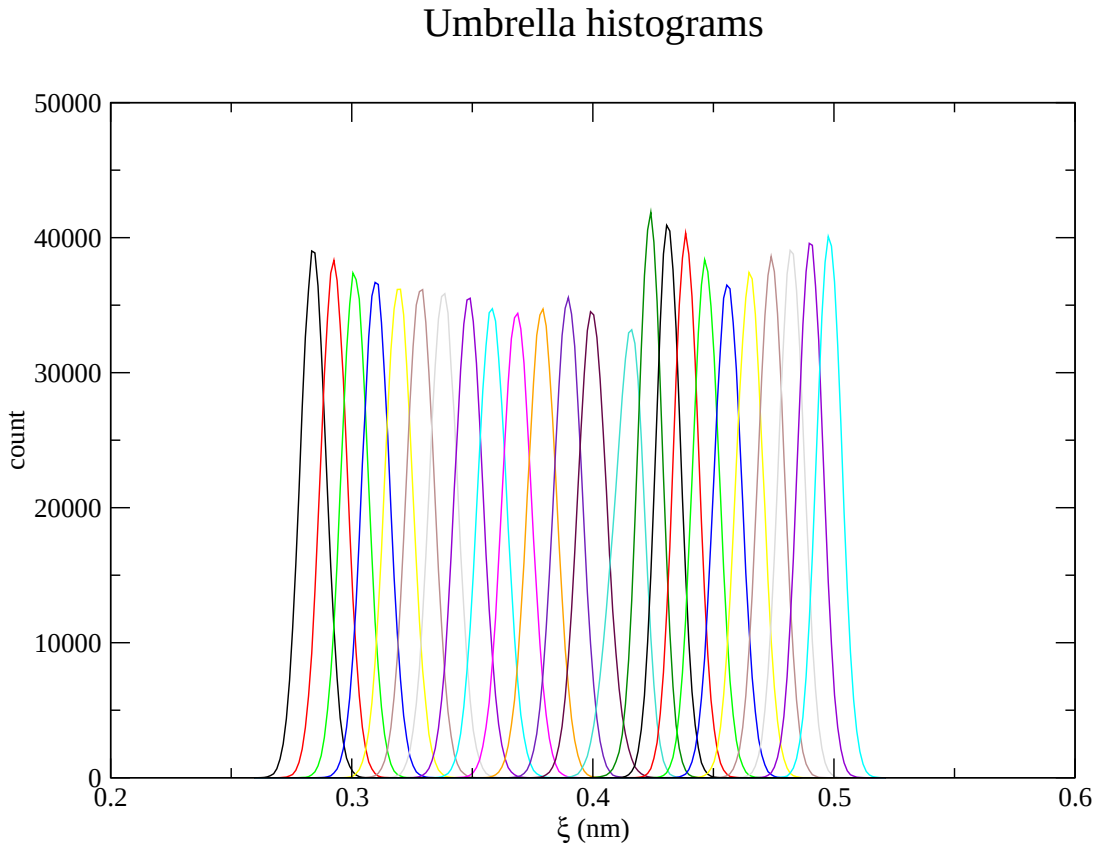

Figure S6: Histrograms of the collective variable in wet IL, O(=P) to O(=C) distance (Å), in each window along the reaction coordinate.

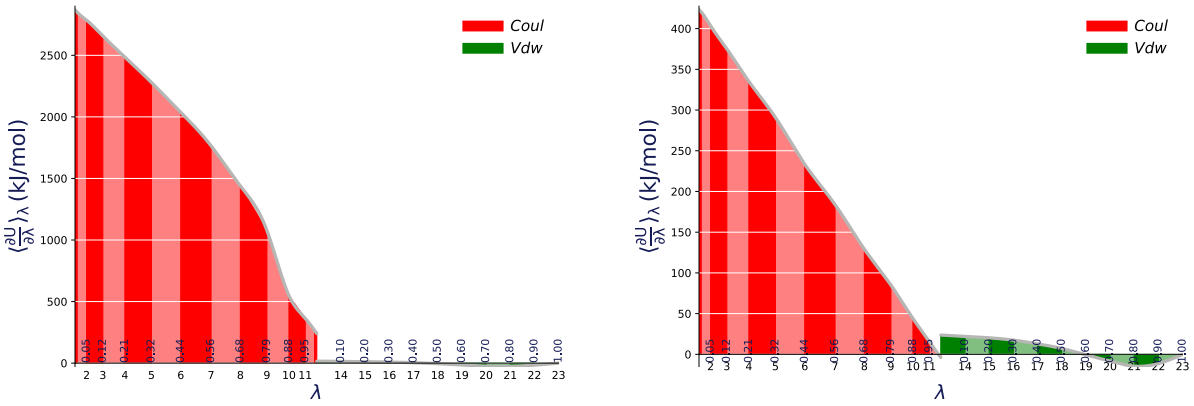

Figure S7: $\langle (\frac{\partial U(\lambda)}{\partial \lambda}) \rangle_{\lambda_i}$ with respect to λ of uranyl (left panel) and nitrate (right panel) in the step (a): the annihilations of uranyl with *cis*-CMPO. Coulombic component is shown by red; VdW component is shown by green; the gray line is the fitted cubic profile in TI-CUBIC methodology.

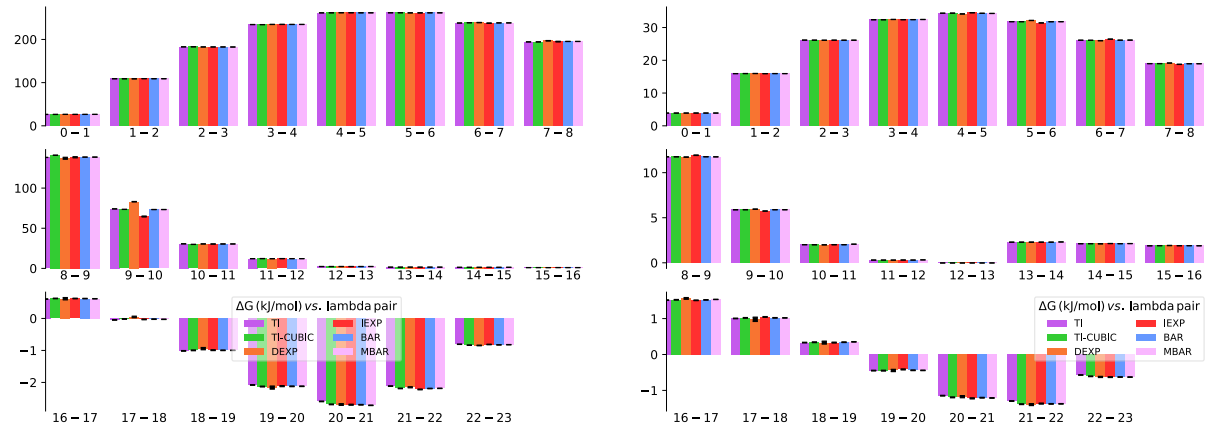

Figure S8: ΔG with respect to each window during the annihilations of uranyl (left panel) and nitrate (right panel) in the step (a): the annihilations of uranyl with *cis*-CMPO.

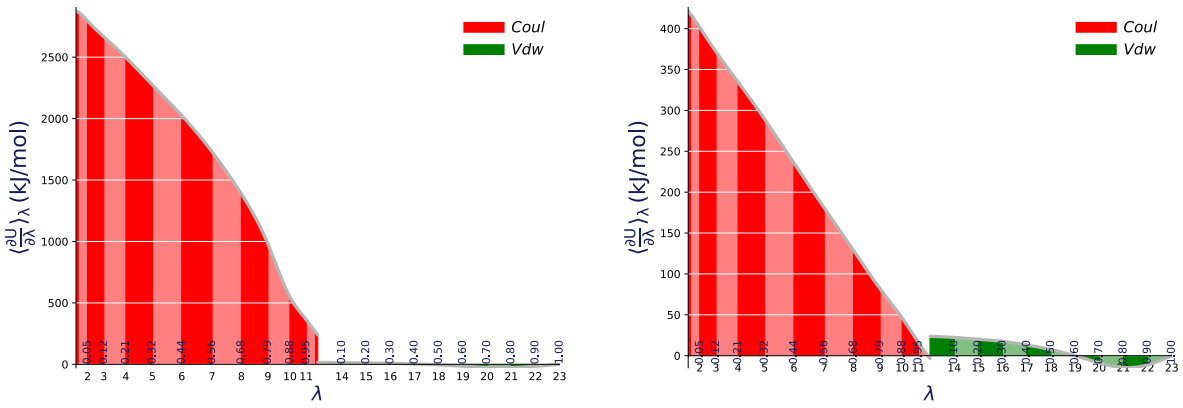

Figure S9: $\langle (\frac{\partial U(\lambda)}{\partial \lambda}) \rangle_{\lambda_i}$ with respect to λ of uranyl (left panel) and nitrate (right panel) in the step (b): the annihilations of uranyl with free CMPO. Coulombic component is shown by red; VdW component is shown by green; the gray line is the fitted cubic profile in TI-CUBIC methodology.

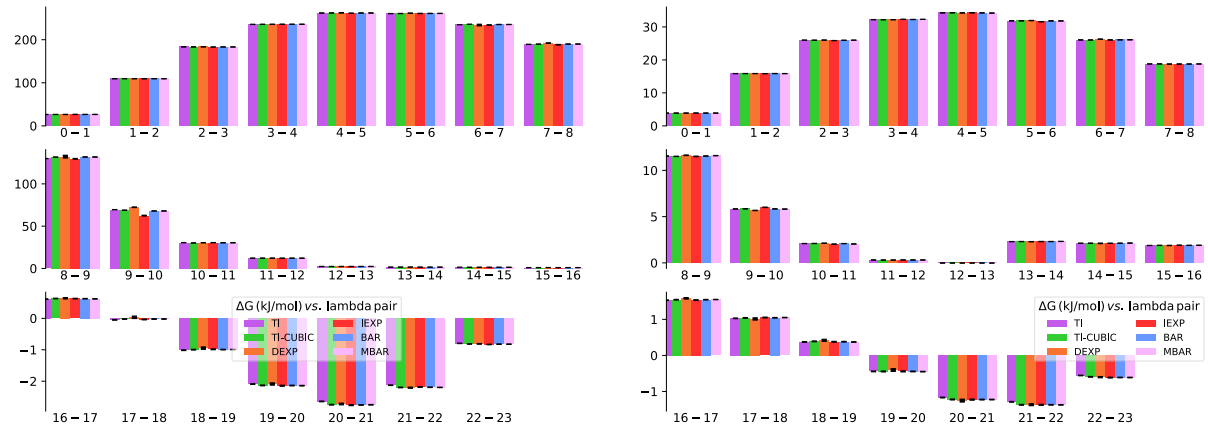

Figure S10: ΔG with respect to each window during the annihilations of uranyl (left panel) and nitrate (right panel) in the step (b): the annihilations of uranyl with free CMPO.

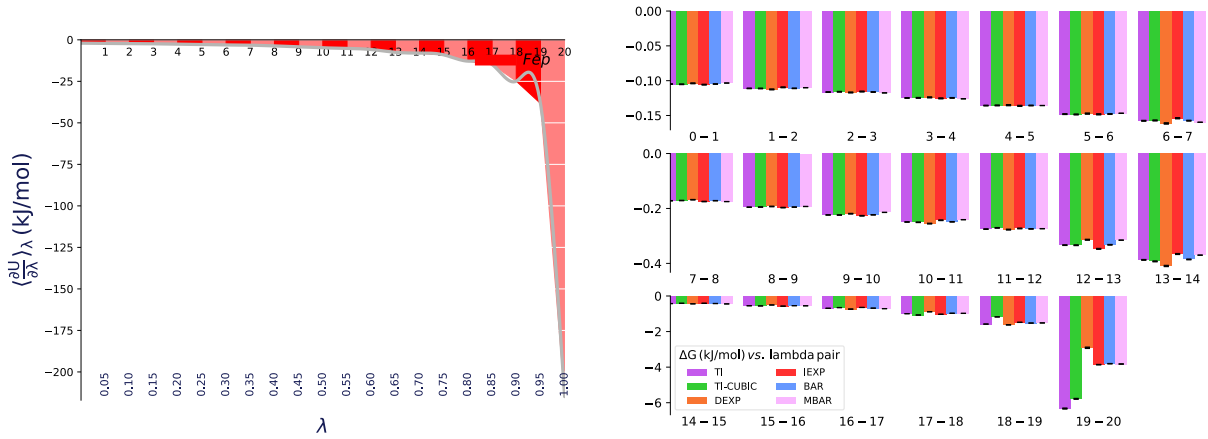

Figure S11: Left panel: $\langle (\frac{\partial U(\lambda)}{\partial \lambda}) \rangle_{\lambda_i}$ with respect to λ in the step (c): the annihilations of restraint on CMPO. Right panel: ΔG with respect to each window.

λ	0	1	2	3	4	5	6	7	8	9	10	11	12	13	14	15	16	17	18	19	20
0	.07	.07	.07	.06	.06	.06	.06	.06	.06	.06	.05	.05	.05	.05	.04	.04	.03	.03	.02	.01	
1	.07	.07	.06	.06	.06	.06	.06	.06	.06	.06	.05	.05	.05	.05	.04	.04	.03	.03	.02	.01	
2	.07	.06	.06	.06	.06	.06	.06	.06	.06	.06	.05	.05	.05	.05	.04	.04	.03	.03	.02	.01	
3	.06	.06	.06	.06	.06	.06	.06	.06	.06	.06	.05	.05	.05	.05	.04	.04	.03	.03	.02	.01	
4	.06	.06	.06	.06	.06	.06	.06	.06	.06	.06	.05	.05	.05	.05	.04	.04	.04	.03	.02	.02	
5	.06	.06	.06	.06	.06	.06	.06	.06	.06	.06	.05	.05	.05	.05	.04	.04	.04	.03	.02	.02	
6	.06	.06	.06	.06	.06	.06	.06	.06	.06	.06	.05	.05	.05	.05	.05	.04	.04	.03	.03	.02	.01
7	.06	.06	.06	.06	.06	.06	.06	.06	.06	.06	.05	.05	.05	.05	.05	.04	.04	.03	.03	.02	.01
8	.06	.06	.06	.06	.06	.06	.06	.06	.06	.05	.05	.05	.05	.05	.05	.04	.04	.04	.03	.02	.01
9	.06	.06	.06	.06	.06	.06	.06	.06	.05	.05	.05	.05	.05	.05	.05	.05	.04	.04	.03	.02	.01
10	.05	.05	.05	.05	.05	.05	.05	.05	.05	.05	.05	.05	.05	.05	.05	.05	.04	.04	.03	.02	.01
11	.05	.05	.05	.05	.05	.05	.05	.05	.05	.05	.05	.05	.05	.05	.05	.05	.05	.04	.04	.03	.01
12	.05	.05	.05	.05	.05	.05	.05	.05	.05	.05	.05	.05	.05	.05	.05	.05	.05	.05	.04	.03	.01
13	.05	.05	.05	.05	.05	.05	.05	.05	.05	.05	.05	.05	.05	.05	.05	.05	.05	.05	.05	.04	.01
14	.04	.04	.04	.04	.04	.04	.05	.05	.05	.05	.05	.05	.05	.05	.06	.06	.06	.06	.05	.04	.02
15	.04	.04	.04	.04	.04	.04	.04	.04	.04	.05	.05	.05	.05	.05	.06	.06	.06	.06	.06	.05	.02
16	.03	.03	.03	.03	.04	.04	.04	.04	.04	.04	.04	.05	.05	.05	.06	.06	.07	.07	.07	.07	.03
17	.03	.03	.03	.03	.03	.03	.03	.03	.04	.04	.04	.04	.05	.05	.06	.06	.07	.08	.09	.09	.05
18	.02	.02	.02	.02	.02	.02	.03	.03	.03	.03	.03	.04	.04	.05	.05	.06	.07	.09	.11	.13	.08
19	.01	.01	.01	.01	.02	.02	.02	.02	.02	.02	.02	.03	.03	.04	.04	.05	.07	.09	.13	.18	.16
20							.01	.01	.01	.01	.01	.01	.01	.01	.02	.02	.03	.05	.08	.16	.55

Figure S12: Overlap matrix of phasing-out the bias potential on CMPO. Darker shades correspond to higher probabilities.

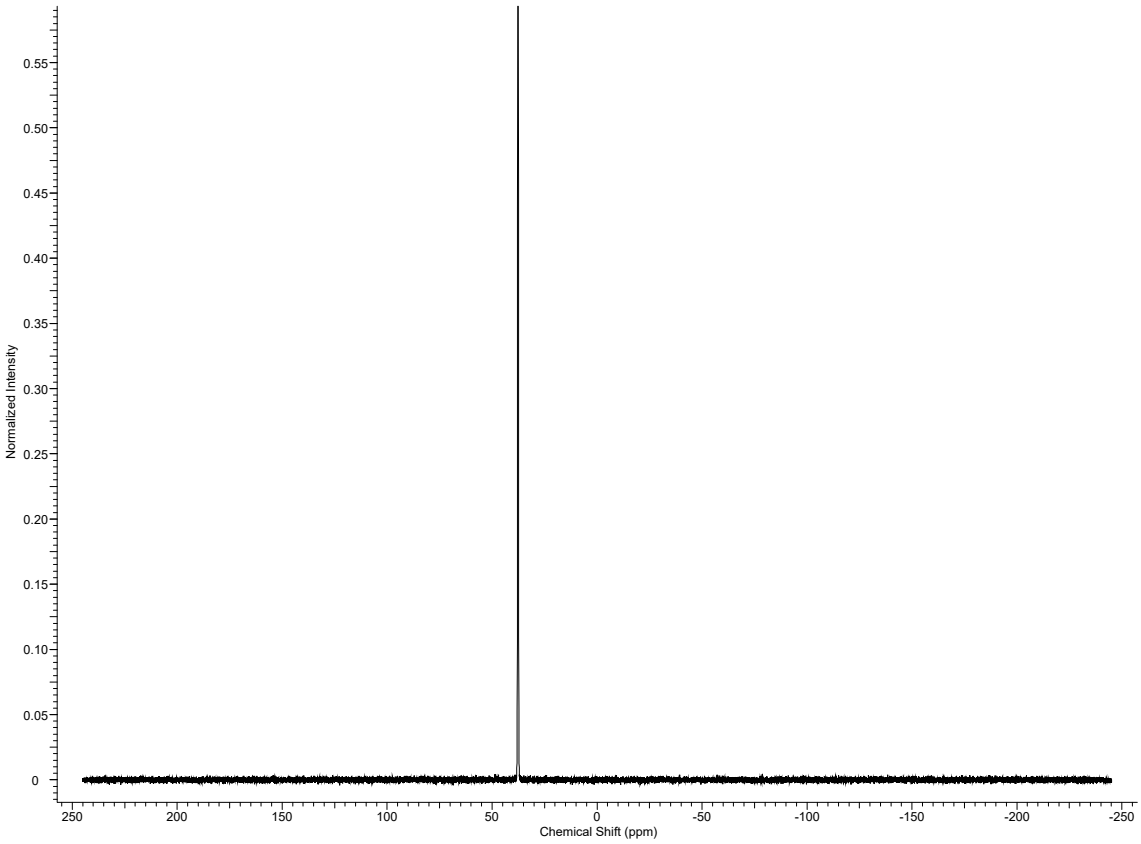

Figure S13: NMR spectra of CMPO in $CDCl_3$ were obtained using a Bruker Avance III 300 spectrometer (300 MHz, ^{1}H; 282.3 MHz, ^{19}F; 121.4 MHz, ^{31}P). Chemical shifts (δ) are reported in parts per million (ppm) relative to tetramethylsilane.

References

(1) Tkac, P.; Vandegrift, G. F.; Lumetta, G. J.; Gelis, A. V. Study of the interaction between HDEHP and CMPO and its effect on the extraction of selected lanthanides. *Industrial & Engineering Chemistry Research* **2012**, *51*, 10433–10444.